Chinese Chemical Letters 33 (2022) 2125–2128

Contents lists available at ScienceDirect

Chinese Chemical Letters

journal homepage: www.elsevier.com/locate/cclet

# Enhanced degradation of organic contaminants by Fe(III)/peroxymonosulfate process with L-cysteine

Chengdu Qi, Yanni Wen, Yijie Zhao, Yinhao Dai, Yanping Li, Chenmin Xu, Shaogui Yang*, Huan He*

*School of Environment, Nanjing Normal University, Nanjing 210023, China*

ARTICLE INFO

*Article history:*
Received 15 September 2021
Revised 19 October 2021
Accepted 29 October 2021
Available online 5 November 2021

*Keywords:*
Advanced oxidation process
Peroxymonosulfate
Fe(II) recycle
L-cysteine
Reactive species
Degradation pathway

ABSTRACT

The difficulty in Fe(III)/Fe(II) conversion in the Fe(III)/peroxymonosulfate (PMS) process limits its efficiency and application. Herein, L-cysteine (Cys), a green natural organic ligand with reducing capability, was innovatively introduced into Fe(III)/PMS to construct an excellent Cys/Fe(III)/PMS process. The Cys/Fe(III)/PMS process, at room temperature, can degrade a variety of organic contaminants, including dyes, phenolic compounds, and pharmaceuticals. In subsequent experiments with acid orange 7 (AO7), the AO7 degradation efficiency followed pseudo-first-order kinetic which exhibited an initial "fast stage" and a second "slow stage". The rate constant values ranged depending on the initial Cys, Fe(III), PMS, and AO7 concentrations, reaction temperature, and pH values. In addition, the presence of $Cl^-$, $NO_3^-$, and $SO_4^{2-}$ had negligible impact while $HCO_3^-$ and humic acid inhibited the degradation of AO7. Furthermore, radical scavenger experiments and methyl phenyl sulfoxide (PMSO) transformation assay indicated that sulfate radical, hydroxyl radical, and ferryl ion (Fe(IV)) were the dominant reactive species involved in the Cys/Fe(III)/PMS process. Finally, based on the results of gas chromatography-mass spectrometry, several AO7 degradation pathways, including N=N cleavage, hydroxylation, and ring opening were proposed. This study provided a new insight to improve the efficiency of Fe(III)/PMS process by accelerating Fe(III)/Fe(II) cycle with Cys.



Recently, advanced oxidation processes (AOPs) involved in highly reactive species, including but not limited to hydroxyl radical ($HO^•$) and sulfate radical ($SO_4^{•-}$), have received increasing attention in destroying refractory organic contaminants in water/wastewater. Compared with classical $HO^•$ based AOPs, the emerging $SO_4^{•-}$ based AOPs has advantages in high redox potential (2.5–3.1 V), long half-life (30–40 μs), and wide operation pH (pH 2.0–8.0) [1]. Peroxymonosulfate (PMS), an important precursor of $SO_4^{•-}$, can be activated by transition metals [2,3], UV [4,5], heat [6], alkali [7] and other catalysts (Eq. 1)[8–11].

$$HSO_5^- \xrightarrow{\text{activators}} SO_4^{•-} + \text{others} \quad (1)$$

Among which transition metals (cobalt and iron) have been proven to effectively initiate the reactive species generation under mild conditions. Although Co has shown superior ability to activate PMS, the inherent toxicity impeded its widely application. Thus, the high effectiveness and environmentally friendly properties of iron make it the most promising PMS activator in application [12]. However, the iron/PMS process still has some disadvantages, such as the difficulty of Fe(II) regeneration, the narrow range of pH and the accumulation of iron sludge, which limit its actual usage [13].

To overcome these negative impacts, reducing agents, such as ascorbic acid, hydroxylamine and metal sulfides, are introduced into the iron activated PMS process to overcome the limitations [14–16]. Compared with aforementioned reducing agents, L-cysteine (Cys) shows superior reducibility and active chelating groups, could relieve the Fe(III) precipitation [17]. In addition, Cys, a naturally occurring amino acid, has no harmful effect on aquatic environment [18,19]. Furthermore, the complex of Fe(III)-Cys may provide a convenient channel for the conversion Fe(III) to Fe(II) [20]. Considering these advantages, Cys could be applied in iron activated PMS process to reduce the precipitation of Fe(III) and accelerate the Fe(III)/Fe(II) conversion. However, to the best of our knowledge, the evaluation of Cys acted as chelating and reducing agents in Fe(III)/PMS process for organic contaminants degradation has never been reported.

In this work, Cys was tentatively introduced into Fe(III)/PMS and the performance of Cys/Fe(III)/PMS process was evaluated for degradation of acid orange (AO7), a typical azo dye which brings

* Corresponding authors.
*E-mail addresses:* yangsg@njnu.edu.cn (S. Yang), huanhe@njnu.edu.cn (H. He).

https://doi.org/10.1016/j.cclet.2021.10.087
1001-8417/

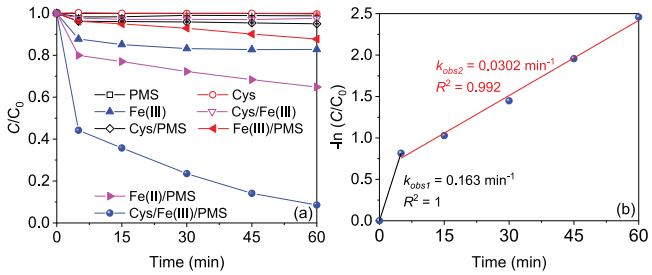


**Fig. 1.** (a) AO7 degradation efficiencies in different processes and (b) kinetics of AO7 degradation in the Cys/Fe(III)/PMS process (reaction conditions: $[AO7]_0$ = 20 μmol/L, $[Cys]_0 = [Fe(III)]_0 = [Fe(II)]_0$ = 0.1 mmol/L, $[PMS]_0$ = 1 mmol/L, $T$ = 25 °C).

serious environmental and ecological problems. Subsequently, the effects of initial Cys, Fe(III), and PMS dosages, initial AO7 concentration, reaction temperature and solution pH on AO7 degradation efficiency were investigated. And then, water constituents including chloride ion, nitrate ion, sulfate ion, bicarbonate ion and humic acid that affected the degradation performance of the Cys/Fe(III)/PMS process were evaluated. In addition, radical scavenger experiments and methyl phenyl sulfoxide (PMSO) transformation assay were conducted to detect the reactive species participated in AO7 degradation. Furthermore, gas chromatography–mass spectrometry (GC–MS) was applied to identify the intermediates of AO7 to deduce the possible degradation pathway.

The chemicals, experimental procedure, and analysis methods are exhibited in Text S1 (Supporting information).

As shown in Fig. 1, the degradation efficiency of AO7 was negligible in the Cys (0.3%), PMS (1.1%), Cys/Fe(III) (2.4%), and Cys/PMS (5.0%) process, which suggest that the abovementioned processes are unreactive toward AO7 [7,21]. When Fe(III) was added, the decolorization efficiency of AO7 was 17.2%, which could be ascribed to the formation of complex AO7-Fe(III) (Fig. S1 in Supporting information) [22]. However, the combination of Fe(III) and PMS, *i.e.*, Fe(III)/PMS process, could only obtain about 12.2% of degradation efficiency of AO7, which could be related to the low activation ability of PMS by Fe(III) [23]. Meanwhile, the degradation efficiency of AO7 could only reach 35.1% in Fe(II)/PMS process. Strikingly, when Cys was introduced into the Fe(III)/PMS process, the decay of AO7 became extremely quick and exhibited a distinct two−stage oxidation process, *i.e.*, an initial fast stage (the first 5 min) followed by a slow one (the post 55 min), which could be contributed to that the introduction of Cys could enhance the Fe(II) generation firstly and then gradually consumption. The degradation efficiency of AO7 rapidly reached to 55.8% in the fast stage within 5 min while then proceeded slowly and obtained 91.4% of removal within 60 min. To further elucidate the degradation process, the *pseudo*−first order kinetic was used to simulate the two−stage reactions and the corresponding rate constants are designated as $k_{obs1}$ and $k_{obs2}$, respectively. As shown in Fig. 1b, the fitted $k_{obs1}$ and $k_{obs2}$ for AO7 degradation were 0.163 $min^{-1}$ and 0.0302 $min^{-1}$, respectively. And the $k_{obs1}$ was 5 times higher than $k_{obs2}$, indicating PMS activation in the Cys/Fe(III)/PMS process was controlled by different processes in these two stages [21,24]. Besides, effects of PS type, iron valent on AO7 degradation and the degradation other organic contaminants were investigated (Text S2 in Supporting information). The above results indicated that the Cys/Fe(III)/PMS process could be employed for removal of various kinds of organic contaminants from wastewater.

As shown in Fig. 2a, the AO7 degradation efficiency increased with the increase in Cys concentration from 0.02 mmol/L to 0.2 mmol/L. However, the further increase of Cys concentration to 0.5 mmol/L resulted in a reduction of AO7 degradation, which could be ascribed to the quenching and scavenging of reactive oxygen species by excess Cys [20,21]. The AO7 degradation efficiency increased with the increase in Fe(III) concentration from 0.02 mmol/L to 0.1 mmol/L (Fig. 2b). However, the continued increasing of Fe(III) concentration from 0.2 mmol/L to 0.5 mmol/L only accelerated the degradation rate of AO7 but had negligible effects on the overall AO7 degradation efficiency, which could be attributed to that the generated amount of Fe(II) from Fe(III) by Cys was stable at the identical Cys concentration and the formation rate of Fe(II) was higher at a higher initial Fe(III) concentration. The AO7 degradation efficiency increased with the increase in PMS concentration from 0.2 mmol/L to 0.5 mmol/L (Fig. 2c). However, the further increase of PMS resulted in the decrease of AO7 degradation, which may be ascribed to the quenching and scavenging of reactive oxygen species by excess PMS [25]. As shown in Fig. 2d, the degradation of AO7 was gradually suppressed as the pH values increased, satisfied AO7 degradation efficiency (76.1%–93.2%) could be obtained at the solution pH range of 3.19–6.17, while AO7 degradation efficiency was reduced to <50% with the higher solution pH (49.5% at pH 7.90 and 41.3% at pH 8.95). Such pH–dependency AO7 degradation could be attributed to the changes in Fe speciation. Although Fe(II) species are readily soluble in the wide pH range of 2–9, the oxidized product Fe(III) will quickly precipitate in the form of ferric oxyhydroxide at pH above 3. The presence of Cys could act as complexing agents toward Fe(III), facilitating the redox cycle of Fe and finally expanding the working pH to 4 [20,21]. In addition, the effect of the AO7 concentration and reaction temperature were evaluated and the results were presented in Text S3 (Supporting information).

As shown in Figs. S5a−c (Supporting information), the existence of chloride ion ($Cl^-$), nitrate ion ($NO_3^-$) or sulfate ion ($SO_4^{2-}$) in the tested concentrations (0.1–5 mmol/L) had a negligible impact on the degradation of AO7, implying the good adaptability of Cys/Fe(III)/PMS process (Text S4 in Support information). However, bicarbonate ($HCO_3^-$) at low concentration (0.1 mmol/L) had a negligible impact, whereas high concentrations (1–5 mmol/L) remarkably suppress AO7 degradation in the Cys/Fe(III)/PMS process Fig. 3a). The degradation efficiency of AO7 decreased from 91.0% to 42.0% within 60 min with increasing $HCO_3^-$ concentration from 0 to 5 mmol/L. The $k_{obs}$, especially the $k_{obs2}$ values declined from 0.0300 $min^{-1}$ to 0.00170 $min^{-1}$ (Fig. S6a in Supporting information). This result could be rationalized by the fact that the addition of $HCO_3^-$ could cause the pH value rise (the solution pH was 3.19, 3.22, 4.70, and 7.01 after adding 0, 0.1, 1, and 5 mmol/L $HCO_3^-$, respectively) which had a negative impact on AO7 degradation and $HCO_3^-$ could reacted with $SO_4^{\bullet-}$ and $HO^\bullet$ to form $HCO_3^{\bullet-}/CO_3^{\bullet-}$ Eqs. 2 and (3) with lower redox potential (1.59 V) and higher selectivity, making it less available for reacting with AO7 [26]. In addition, humic acid (HA), a representative natural organic matter, significantly inhibited the degradation of AO7 in the Cys/Fe(III)/PMS process with the tested concentrations (0.1–5 mg/L) (Fig. 3b). The degradation efficiency of AO7 decreased from 87.9% to 67.8% with increasing HA concentration from 0 to 5 mg/L. The $k_{obs}$, especially the $k_{obs1}$ values declined from 0.161 $min^{-1}$ to 0.0588 $min^{-1}$ (Fig. S6b in Supporting information). This result could be explained by the fact that HA competitively reacted with $SO_4^{\bullet-}$ and $HO^\bullet$ (Eq. 4), making it less available for reacting with AO7 [27].

$$CO_3^{2-} + SO_4^{\bullet-}(HO^\bullet) \rightarrow CO_3^{\bullet-} + SO_4^{2-}(OH^-) \quad (2)$$

$$HCO_3^- + SO_4^{\bullet-}(HO^\bullet) \rightarrow HCO_3^{\bullet-} + SO_4^{2-}(OH^-) \quad (3)$$

$$HA + SO_4^{\bullet-}(HO^\bullet) \rightarrow HA_{products} + SO_4^{2-}(OH^-) \quad (4)$$

$SO_4^{\bullet-}$ and $HO^\bullet$ are recognized as the primary reactive oxygen species involved in various activated PMS processes. In order to identify the reactive oxygen species involved in the Cys/Fe(III)/PMS

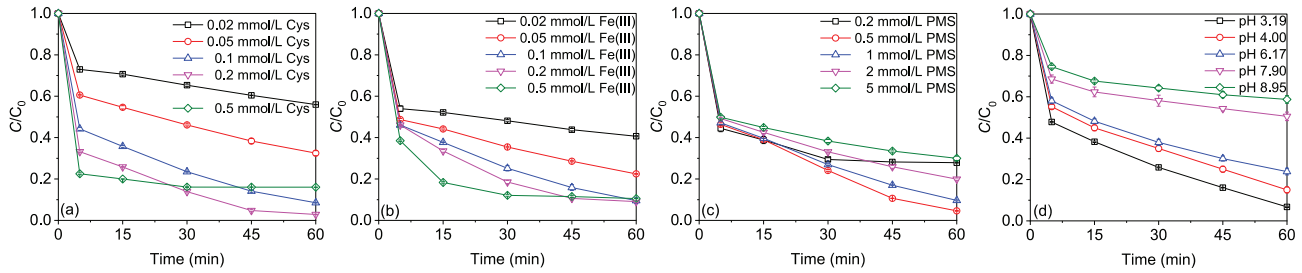


**Fig. 2.** Effect of (a) Cys-concentration, (b) Fe(III) concentration, (c) PMS concentration, and (d) solution pH on AO7 degradation efficiencies in the Cys/Fe(III)/PMS process (Except for the investigated parameter, the other parameters were fixed at: $[AO7]_0$ = 20 μmol/L, $[Cys]_0 = [Fe(III)]_0$ = 0.1 mmol/L, $[PMS]_0$ = 1 mmol/L, pH 3.19, $T$ = 25 °C).

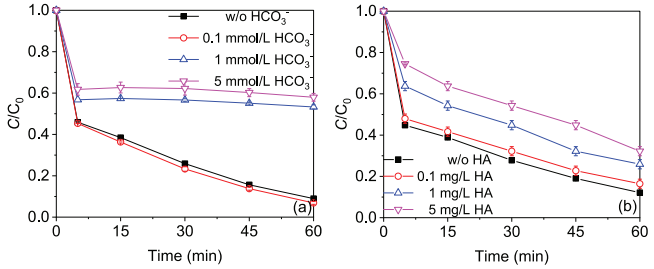


**Fig. 3.** Effect of (a) $HCO_3^-$ and (b) humic acid on AO7 degradation efficiencies in the Cys/Fe(III)/PMS process (reaction conditions: $[AO7]_0$ = 20 $\mu$mol/L, $[Cys]_0 = [Fe(III)]_0$ = 0.1 mmol/L, $[PMS]_0$ = 1 mmol/L, $T$ = 25 °C).

process, radical quenching experiment was performed by adding different amounts of TBA and EtOH, respectively. EtOH usually acts as a scavenger for both $SO_4^{\bullet-}$ and HO• ($k_{EtOH,\ HO^\bullet}$ = (1.8–2.8) × $10^9$ L $mol^{-1}$ $s^{-1}$, $k_{EtOH,\ SO_4^{\bullet-}}$ = (1.6–7.7) × $10^7$ L $mol^{-1}$ $s^{-1}$) while TBA for HO• ($k_{TBA,\ HO^\bullet}$ = (3.8–7.6) × $10^8$ L $mol^{-1}$ $s^{-1}$, $k_{TBA,\ SO_4^{\bullet-}}$ = (4.0–9.1) × $10^5$ L $mol^{-1}$ $s^{-1}$). As shown in Fig. 4a, 91.5% of AO7 was degraded in the absence of radical scavengers. However, AO7 degradation efficiencies were suppressed with different dosages of TBA or EtOH addition, indicating that $SO_4^{\bullet-}$ and HO• might be the dominating reactive oxygen species. When 0.1 mol/L TBA was added, the degradation efficiency of AO7 decreased to 76.7%, indicating 16.2% of the degradation inhibition occurred because of HO•. As the concentration of TBA increased to 0.5 mol/L, the degradation efficiency of AO7 reduced significantly to 58.1%. It has fully been proven that the enhancement restraint of target organic contaminant removal may due to the scavenging of TBA with both the $SO_4^{\bullet-}$ and HO• other than the HO• alone, especially with a high TBA level. Thus, 0.1 mol/L TBA was appropriate for completely scavenging of HO• in the present study. In the presence of 0.1 mol/L EtOH, the degradation efficiency of AO7 decreased to 52.6%. As the dosage of EtOH increased to 0.5 mol/L, the degradation efficiency of AO7 reduced to 23.9%, showing 0.5 mol/L EtOH was appropriate for completely scavenging of $SO_4^{\bullet-}$ and HO• and 57.7% of the degradation restraint happened because of $SO_4^{\bullet-}$. The remaining 26.1% of degradation efficiency of AO7 may due to other reactive species (*e.g.*, PMS and $SO_4^{\bullet-}$).

It has been reported that Fe(IV) could be produced in iron activated PMS process [28]. To explore the possible existence of Fe(IV) in the Cys/Fe(III)/PMS process, PMSO was used as the probe compound as Fe(IV) could selectively transform PMSO to a unique oxygen product $PMSO_2$, which was different from the radical–induced byproducts. As shown in Fig. 4b, the concentration of produced $PMSO_2$ was 30 μmol/L and the concentration of PMSO decreased by 40 μmol/L after 60 min, indicating that Fe(IV) was generated in the Cys/Fe(III)/PMS process. Moreover, the yield of $PMSO_2$, which means the molar ratio of $PMSO_2$ produced to PMSO lost, can be used to evaluate the contribution of Fe(IV) to PMSO degradation. In this study, the yield of $PMSO_2$ was identified as 70.8%–73.3% during the reaction period (Fig. 4b). The yield below 100% may be due to the PMSO degradation caused by reactive oxygen species generated [29]. To sum up, Fe(IV) could be also presented in the Cys/Fe(III)/PMS process.

In addition, the effect of oxygen on AO7 degradation in the Cys/Fe(III)/PMS process was investigated by purging air or nitrogen. As depicted in Fig. 4c, the degradation efficiency of AO7 was high (around 90%) in the atmosphere rich in oxygen, while the decolorization was strongly retarded to 47.8% in the absence of oxygen (purging nitrogen). Besides, the concentration of dissolved oxygen (DO) were monitored and DO kept stable during the degradation process (Fig. S7 in Supporting information). This could be ascribed to the evolution of $O_2^{\bullet-}$ in the presence of oxygen. Fe(II) generated from the reduction of Fe(III) by Cys could react with oxygen to form $O_2^{\bullet-}$, which would quickly activate $HSO_5^-$ to generate $SO_4^{\bullet-}$ [24]. Owing to this additional activation pathway, reactive oxygen species would be continuously generated and consequently promote the degradation of AO7.

Based on the aforementioned results, we assumed that the introduction of Cys into the Fe(III)/PMS process significantly accelerated the transformation from Fe(III) to Fe(II) and thus generated more reactive species and improved the oxidation efficiency. To verify our hypothesis, the variation of Fe(II), Cys and PMS concentration with time in the Cys/Fe(III)/PMS process was monitored. As shown in Fig. 4d, Fe(II) was rapidly generated along with the addition of Cys in the first 5 min. It has been reported that the sulfhydryl group (–SH) in Cys could act as electron donor to transform the Fe(III) into Fe(II) (Li *et al.*, 2016). And then, the concentration of Fe(II) decreased gradually with the proceeding of AO7 degradation. Besides, the degradation of AO7 was almost suppressed (5.9% removal efficiency) in Fe(II)/PMS process with 0.1 mmol/L EDTA (Fig. S8 in Supporting information), a strong Fe(II) chelator, which proved the importance role of Fe(II) in the Cys/Fe(III)/PMS process for AO7 degradation. Meanwhile, the level of Cys was also reduced gradually, which could be associated with the reaction between Cys and Fe(III) for the regeneration of Fe(II) [21]. The decay pattern of PMS was similar to that of Cys, which could be attributed with the reaction between PMS and the regenerated Fe(II) [13].

Combined with the above results, the activation mechanism of the Cys/Fe(III)/PMS process could be tentatively proposed (Scheme S1 in Supporting information). Serving as electron donor, Cys converted to Cystine which accompanied with transferring electrons to Fe(III), triggered the redox cycle of Fe(III)/Fe(II) and resulted in the regeneration of Fe(II) Eq. 5). And then, PMS was activated Fe(II) with the formation of $SO_4^{\bullet-}$ and HO• (Eqs. 6 and (7). Besides, HO• can also be formed through the reactions of $SO_4^{\bullet-}$ with $H_2O/OH^-$ (Eq. 8). In addition, the reaction of Fe(II) and PMS can generate Fe(IV) (Eq. 9), which was finally converted to Fe(III) via secondary reactions with Fe(II), $H_2O$ or PMS (Eq. 10) [13]. Meanwhile, a portion of Cys could regenerated by the reaction between

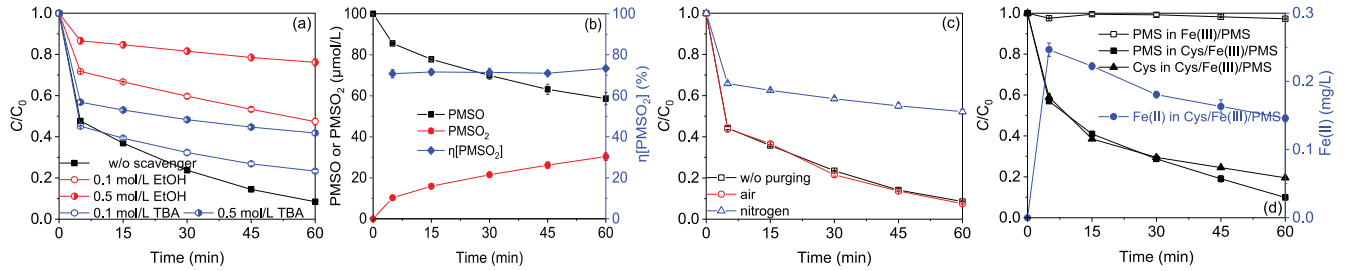


**Fig. 4.** Effect of (a) radical scavengers, (c) dissolved oxygen on AO7 degradation efficiencies, (b) PMSO loss, $PMSO_2$ generation, and $\eta[PMSO_2]$ values in the Cys/Fe(III)/PMS process. (d) Changes of Fe(II), Cys-and PMS in the Fe(III)/PMS and Cys/Fe(III)/PMS processes (reaction conditions: $[AO7]_0$ = 20 μmol/L or $[PMSO]_0$ = 100 μmol/L, $[Cys]_0 = [Fe(III)]_0$ = 0.1 mmol/L, $[PMS]_0$ = 1 mmol/L, $T$ = 25 °C).

Cystine and HO• (Eq. 11) [19,30]. It should be noted that in this process, Fe(II) was continuously regenerated by Cys and then was consumed by PMS, generating multiple reactive species and consequently degrading AO7.

$$2Cys + 2Fe(III) \rightarrow 2Fe(II) + Cystine + 2H^+ \quad (5)$$

$$Fe(II) + HSO_5^- \rightarrow Fe(III) + SO_4^{\bullet -} + OH^- \quad (6)$$

$$Fe(II) + HSO_5^- \rightarrow Fe(III) + SO_4^{2-} + HO^{\bullet} \quad (7)$$

$$SO_4^{\bullet -} + H_2O/OH^- \rightarrow SO_4^{2-} + HO^{\bullet} \quad (8)$$

$$Fe(II) + HSO_5^- \rightarrow Fe^{IV}O^{2+} + SO_4^{2-} + H^+ \quad (9)$$

$$Fe^{IV}O^{2+} + Fe(II)/H_2O/HSO_5^- \rightarrow Fe(III) + others \quad (10)$$

$$Cystine + HO^{\bullet} \rightarrow Cys + OH^- \quad (11)$$

Furthermore, AO7 degradation pathways were proposed based on the results of gas chromatography-mass spectrometry (Text S5 in Supporting information).

To sum up, Cys was successful proved to have the enhancement impact for the degradation of AO7 in the Fe(III)/PMS process and the AO7 degradation exhibited a distinct two−stage oxidation process, *i.e.*, an initial fast stage followed by a slow one. Besides dyes, phenolic compounds and pharmaceuticals can also be degraded in the Cys/Fe(III)/PMS process. The AO7 degradation efficiency increased with the increase in Cys, Fe(III) concentration, and reaction temperature. However, the superfluous PMS was not favor for the AO7 degradation. The higher the pH was applied, the poor degradation of AO7 was observed. The existence of $Cl^-$, $NO_3^-$ or $SO_4^{2-}$ had a negligible impact while $HCO_3^-$ and humic acid inhibited on the degradation of AO7. Sulfate radical, hydroxyl radical, and ferryl ion (Fe(IV)) were deduced as the dominant reactive species involved in the Cys/Fe(III)/PMS process by the results of radical scavenger experiments and methyl phenyl sulfoxide (PMSO) transformation assay. N=N cleavage, hydroxylation, and ring opening were proposed as AO7 degradation pathways based on the results of GC-MS.

## Declaration of competing interest

The authors declare that they have no known competing financial interests or personal relationships that could have appeared to influence the work reported in this paper.

## Acknowledgments

This work was supported by the Natural Science Foundation of Jiangsu Province , China (No. BK20200721), the Natural Science Foundation of the Higher Education Institutions of Jiangsu Province, China (No. 19KJB610016), the National Natural Science Foundation of China (No. 21777067), the Six Talent Peaks Project in Jiangsu Province, China (No. JNHB–10), and Primary Research & Development Plan of Jiangsu Province, China (No. BE2019743). The authors would like to thank Xueyan Liu from Shiyanjia Lab (www.shiyanjia.com) for the GC-MS analysis.

## Supplementary materials

Supplementary material associated with this article can be found, in the online version, at doi:10.1016/j.cclet.2021.10.087.

## References

[1] C. Wang, R. Huang, R. Sun, J. Yang, M. Sillanpää, J. Environ. Chem. Eng. 9 (2021) 106267.
[2] G.P. Anipsitakis, D.D. Dionysiou, Environ. Sci. Technol. 38 (2004) 3705–3712.
[3] P. Hu, M. Long, Appl. Catal. B: Environ. 181 (2016) 103–117.
[4] G.P. Anipsitakis, D.D. Dionysiou, Appl. Catal. B: Environ. 54 (2004) 155–163.
[5] Y.H. Guan, J. Ma, X.C. Li, J.Y. Fang, L.W. Chen, Environ. Sci. Technol. 45 (2011) 9308–9314.
[6] C. Qi, X. Liu, C. Lin, et al., Chem. Eng. J. 315 (2017) 201–209.
[7] C. Qi, X. Liu, J. Ma, et al., Chemosphere 151 (2016) 280–288.
[8] P. Duan, Y. Qi, S. Feng, et al., Appl. Catal. B: Environ. 267 (2020) 118717.
[9] L. Peng, X. Duan, Y. Shang, B. Gao, X. Xu, Appl. Catal. B: Environ. 287 (2021) 119963.
[10] Y. Shang, X. Duan, S. Wang, et al., Chin. Chem. Lett. 33 (2022) 663–673.
[11] Y. Shang, X. Xu, B. Gao, S. Wang, X. Duan, Chem. Soc. Rev. 50 (2021) 5281–5322.
[12] S. Xiao, M. Cheng, H. Zhong, et al., Chem. Eng. J. 384 (2020) 123265.
[13] X. Li, J. Ma, Y. Gao, et al., Chem. Eng. J. 427 (2022) 131995.
[14] H. Zhou, H. Zhang, Y. He, B, et al., Appl. Catal. B: Environ. 286 (2021) 119900.
[15] D. Yuan, C. Zhang, S. Tang, et al., Chin. Chem. Lett. 32 (2021) 3387–3392.
[16] M. Zhao, Y. Xiang, X. Jiao, et al., Sep. Purif. Technol. 276 (2021) 119289.
[17] J. Lu, T. Wang, Y. Zhou, et al., J. Hazard. Mater. 383 (2020) 121133.
[18] L. Luo, Y. Yao, F. Gong, et al., RSC Adv. 6 (2016) 47661–47668.
[19] T. Li, Z. Zhao, Q. Wang, P. Xie, J. Ma, Water Res. 105 (2016) 479–486.
[20] W. Huang, B. Fu, S. Fang, et al., Sci. Total Environ. 793 (2021) 148555.
[21] F. Jiang, Y. Li, W. Zhou, et al., Chem. Eng. J. 387 (2020) 124048.
[22] H. Park, W. Choi, J. Photochem. Photobiol. A 159 (2003) 241–247.
[23] H. Song, D. Zu, C. Li, et al., Chem. Eng. J. 423 (2021) 130012.
[24] T. Pan, Y. Wang, X. Yang, X.F. Huang, R.L. Qiu, Chem. Eng. J. 384 (2020) 123248.
[25] G. Peng, C. Qi, X. Wang, et al., Chemosphere 266 (2021) 128944.
[26] J. Wang, S. Wang, Chem. Eng. J. 411 (2021) 128392.
[27] C. Qi, G. Yu, J. Huang, et al., Chem. Eng. J. 353 (2018) 490–498.
[28] X. Li, X. Liu, C. Lin, et al., Chem. Eng. J. 382 (2020) 123013.
[29] Z. Wang, W. Qiu, S. Pang, et al., Water Res. 172 (2020) 115504.
[30] D.Q. He, Y.J. Zhang, D.N. Pei, et al., J. Hazard. Mater. 382 (2020) 121090.